



OPEN ACCESS

EDITED BY

Sushant K. Singh,
CAIES Foundation, India

REVIEWED BY

Sandeep Samantaray,
National Institute of Technology Srinagar, India
Nasrin Fathollahzaddeh Attar,
University of Tabriz, Iran

*CORRESPONDENCE

Fan Feng,
✉ fanfeng2023@163.com
Hamzeh Ghorbani,
✉ hamzehghorbani68@yahoo.com

RECEIVED 09 September 2023

ACCEPTED 05 February 2024

PUBLISHED 16 February 2024

CITATION

Feng F, Ghorbani H and Radwan AE (2024),
Predicting groundwater level using traditional
and deep machine learning algorithms.
Front. Environ. Sci. 12:1291327.
doi: 10.3389/fenvs.2024.1291327

COPYRIGHT

© 2024 Feng, Ghorbani and Radwan. This is an
open-access article distributed under the terms
of the [Creative Commons Attribution License
\(CC BY\)](https://creativecommons.org/licenses/by/4.0/). The use, distribution or reproduction in
other forums is permitted, provided the original
author(s) and the copyright owner(s) are
credited and that the original publication in this
journal is cited, in accordance with accepted
academic practice. No use, distribution or
reproduction is permitted which does not
comply with these terms.

Predicting groundwater level using traditional and deep machine learning algorithms

Fan Feng^{1*}, Hamzeh Ghorbani^{2*} and Ahmed E. Radwan³

¹University of Applied Sciences for Engineering and Economics, Berlin, Germany, ²Young Researchers and Elite Club, Ahvaz Branch, Islamic Azad University, Ahvaz, Iran, ³Faculty of Geography and Geology, Institute of Geological Sciences, Jagiellonian University, Kraków, Poland

This research aims to evaluate various traditional or deep machine learning algorithms for the prediction of groundwater level (GWL) using three key input variables specific to Izeh City in the Khuzestan province of Iran: groundwater extraction rate (E), rainfall rate (R), and river flow rate (P) (with 3 km distance). Various traditional and deep machine learning (DML) algorithms, including convolutional neural network (CNN), recurrent neural network (RNN), support vector machine (SVM), decision tree (DT), random forest (RF), and generative adversarial network (GAN), were evaluated. The convolutional neural network (CNN) algorithm demonstrated superior performance among all the algorithms evaluated in this study. The CNN model exhibited robustness against noise and variability, scalability for handling large datasets with multiple input variables, and parallelization capabilities for fast processing. Moreover, it autonomously learned and identified data patterns, resulting in fewer outlier predictions. The CNN model achieved the highest accuracy in GWL prediction, with an RMSE of 0.0558 and an R^2 of 0.9948. It also showed no outlier data predictions, indicating its reliability. Spearman and Pearson correlation analyses revealed that P and E were the dataset's most influential variables on GWL. This research has significant implications for water resource management in Izeh City and the Khuzestan province of Iran, aiding in conservation efforts and increasing local crop productivity. The approach can also be applied to predicting GWL in various global regions facing water scarcity due to population growth. Future researchers are encouraged to consider these factors for more accurate GWL predictions. Additionally, the CNN algorithm's performance can be further enhanced by incorporating additional input variables.

KEYWORDS

groundwater level, deep machine learning, CNN algorithm, prediction, water management

1 Introduction

The groundwater level (GWL) is of critical importance, especially in arid and semi-arid countries (Alfarrah and Walraevens, 2018; Bovolo et al., 2009; Priyan, 2021). In many areas, the overexploitation of GWL has led to irreparable damage to the groundwater sources (Alfarrah and Walraevens, 2018; Bovolo et al., 2009; Priyan, 2021). Predicting GWL is a key challenge in hydrogeological investigations, effective aquifer management, and assessment of subterranean water volume (Sun et al., 2022; Barzegar et al., 2017). Hydrogeological studies have been conducted to estimate the potential of underground water, predict changes in the GWL, and examine the current state of underground water resources (Hay

and Mimura, 2005; Russo and Taddia, 2009). Empirical time series models have been extensively used to predict GWL levels (Eriksson, 1970). The ability of empirical or numerical models such as finite element groundwater flow system (FEFLOW)¹ (Ma et al., 2022), modular finite-difference flow model (MODFLOW)² (Hughes et al., 2022), and HydroGeoSphere³ (Kang et al., 2017) to estimate the GWL has made these models helpful in predicting the GWL (Trefry and Muffels, 2007; Wang et al., 2008; Brunner and Simmons, 2012).

1.1 Problem statement

The prediction of GWL is crucial for sustainable water resource management, as accurate forecasts contribute to understanding the availability and distribution of groundwater, essential for purposes such as agriculture, drinking water supply, and ecosystem maintenance (Singh et al., 2021a; Pragnaditya et al., 2021; Khan et al., 2023). Machine learning (ML) techniques offer the potential to analyze large and complex datasets, identify patterns, and make predictions that inform decision-making in water resource management (Singh, 2015; Singh et al., 2021b; Pham et al., 2022; Ghobadi and Kang, 2023; Singh et al., 2024). By applying ML to predict GWL, we can enhance our ability to monitor and manage water resources effectively, ensuring their sustainable use over time (Tao et al., 2022a; Pham et al., 2022). However, in Izeh City, Khuzestan province of Iran, certain challenges, such as low rainfall, increasing temperature, consecutive droughts, and overexploitation of GWL for agricultural purposes, create gaps in the prediction of GWL for this region. The absence of accurate predictive models tailored to Izeh City's unique context poses a significant obstacle to achieving reliable predictions. Addressing these challenges is crucial for developing robust ML models that accurately forecast GWL in the region, thereby facilitating more effective water resource management strategies.

1.2 Literature review

Using the mathematical model of the aquifer is one of the best methods for managing and controlling the drop in water levels (Rajaei et al., 2019). In GWL mathematical models, differential equations are utilized to simulate GWL flow (Rajaei et al., 2019). Since the dynamic behavior of a hydrological system changes with the passage of time, the indicated models do not have adequate ability to predict the characteristics of water resources and are not suitable models (Rathinasamy et al., 2014). Physical models

generally excel at capturing and delineating the relationships between variables, as they are built upon established scientific principles and laws. These models are grounded in a fundamental understanding of the underlying processes and mechanisms governing the system under consideration. This allows physical models to provide valuable insights into the behavior and interactions of various components within the system. Since the relationships between the variables affecting the GWL are complex and non-linear, physical models in practice require a lot of data to simulate the fluctuations of the GWL (Nayak et al., 2006; Khan and Valeo, 2016). Deep learning models, while powerful in terms of prediction performance, are often considered black-box models with limited interpretability, making it challenging to understand the exact relationships between variables. Based on artificial neural network (ANN), these models have shown remarkable success in various fields, such as image recognition, natural language processing, and gameplay (Nadiri et al., 2013).

Researchers have developed innovative approaches to predict the water level in aquifers in light of the numerous issues with artificial models for modeling aquifers (Tao et al., 2022b). Artificial intelligence (AI) models have been applied in a number of areas recently, including hydrogeological and underground water research (Nadiri et al., 2014). AI algorithms can use sparse, brief data to mimic irregular and non-linear time series with high accuracy. Due to their accuracy and usefulness, these models have been employed in recent years to anticipate the GWL (Franses and Van Dijk, 2000). Gong et al. (2015) tested the validity of three nonlinear time-series intelligence models, namely ANN, support vector machine (SVM), and adaptive neuro-fuzzy inference system (ANFIS), for the prediction of GWL considering surface water-groundwater interaction. The models were applied to two wells near Lake Okeechobee in Florida, United States, using a 10-year dataset of hydrological parameters. Evaluation measures showed that the ANFIS and SVM models provided more accurate predictions than the ANN model. Taking into account the surface water-groundwater interaction improved the prediction accuracy, particularly in areas close to the surface water, such as the lake area (Gong et al., 2016). Wen et al. (2017) introduced the wavelet analysis-artificial neural network (WA-ANN) model to predict the GWL in China for the next 1, 2, and 3 months. GWL, climate data, and water level were taken into consideration as input data in this study. They concluded that the suggested model is most accurate when the previous GWL is used as input data. In conclusion, it can be claimed that the WA-ANN model is a reliable and effective tool for estimating GWL (Wen et al., 2017). Kaya et al. (2018) used 196 data points from 2000 to 2015 to predict the GWL in the Turkish province of Reyhanli. They applied ANN and M5tree (M5T) model approaches in their investigation. They claimed that the methodologies suggested in this study are remarkably accurate for estimating the GWL and that the approaches presented in this study perform effectively (Kaya et al., 2018). Zhang et al. (2018) developed a Long short-term memory (LSTM) time series model to predict water table depth in agricultural areas with complex hydrogeological characteristics. Their proposed model outperformed the traditional feed-forward neural network (FFNN) in GWL prediction, achieving higher R^2 scores (0.789–0.952). The dropout method effectively prevented overfitting, and the model's architecture demonstrated a strong learning ability on time series data. The study suggests that the

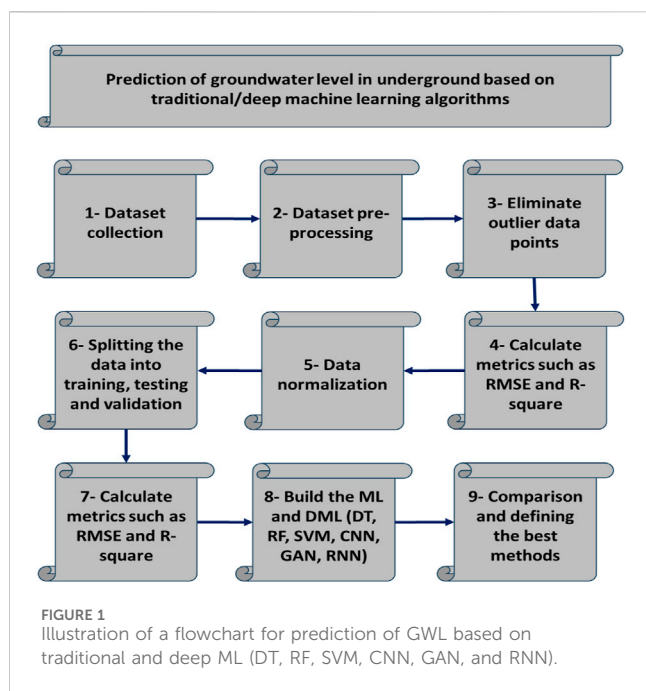
1 FEFLOW: is a computer program for simulating groundwater flow, mass transfer, and heat transfer in porous and fractured media

2 MODFLOW: is the U.S. Geological Survey modular finite-difference flow model, which is a computer code that solves the groundwater flow equation.

3 HydroGeoSphere: is a 3D control-volume finite element groundwater model that accounts for surface and subsurface flow, solute and energy transport, and heat transport.

TABLE 1 List of the previous work on the prediction of the GWL based on DML.

References	Study year	Study region	Sample size and data range	ML/DL modeling method used	Model performance	
					RMSE	R ²
Gong et al	2015	United States	A dataset of monthly records for 12 years and 10 years of data are used for training and the second 2 years' data are used for validation	ANN, SVM, and ANFIS	1.112	0.931
Wen et al	2017	China	Dataset of monthly records for 7.5 years, a dataset from 2003/6–2008/12 were assigned for the training, and the values of 2009/1–2010/12 for testing	WA-ANN	0.109	0.973
Zhang et al	2018	China	Dataset of monthly records for 14 years, the first 12 years of time series data were used as a training set, and the next 2 years of data were used as a validation set	DNN, LSTM, Double-LSTM	0.070	0.952
Kaya, et al	2018	Turkey	Dataset of monthly records for 16 years, total of 192, 144 data of 192 were used for training and 48 data were analyzed for the test	ANN, M5T	2.050	0.892
Kombo, et al	2020	Rwanda	Dataset of daily records for 2 years. The training and validation percentages for 90-day-ahead (t + 90) the used prediction horizons were (98.0237% and 1.9763%) respectively	KNN-RF, ANN, KNN, SVM, RF	0.220	0.979
Kumar et al	2020	Japan	Dataset of 84 data samples for 70 months, the training dataset (70% of total data), and the testing dataset (30% of total data)	ELM-GPR	0.080	0.950
Sharafati et al	2020	Iran	Dataset of monthly records for 10 years, the training dataset (75% of total data), and the testing dataset (25% of total data)	GBR	0.088	0.940
Banadkooki et al	2020	Iran	Dataset of monthly records for 13 years, the training dataset (70% of total data), and the testing dataset 30% of total data)	MLP-WA, RBF-WA, GP	0.300	0.930
Osman et al	2021	Malaysia	Dataset of daily data records for 9 months, the training dataset (70% of total data), and the testing dataset 30% of total data)	Xgboost, ANN, SVR	0.138	0.920
Malakar et al	2021	India	The dataset of data records for 23 years was collected four times per year; the total GWL dataset of 23 years (23 × 4 = 92 seasons, 1996–2018) is split into two parts: the training set (1996–2013, 18 years) and the testing data set (2014–2018, 5 years) and finally predicted GWL for the next 5 years (2019–2023)	FNN, RNN, LSTM	0.490	0.920
Afan et al	2021	Malaysia	Dataset of daily basis records from 2017 until mid of 2018, the training dataset (70% of total data), and the testing dataset (30% of total data)	DL, EDL	0.145	0.790
Dehghani et al	2022	Iran	Dataset of monthly records for 11 years, the training dataset (70% of total data), and the testing dataset (30% of total data)	ANN, BWO, AIG, CSO	0.710	0.995
Khan et al	2023	World wide	Dataset records of 109 articles with data records for 15 years, data processing, and the separation of training and testing are not included in the Analysis	DL, ML	-	-
Mohammed et al	2023	Sonqor	Dataset records of 306 months, training dataset (70% of total data), and the testing dataset (30% of total data)	GA-ANN, GA-ICA, ELM, ORELM	0.420	0.916



LSTM-based model can be a valuable alternative for the prediction of GWL, particularly in data-scarce areas (Zhang et al., 2018). Kombo et al. (2020) introduced the K-Nearest Neighbour-random forest (KNN-RF) model along with ANN, KNN, SVM, and RF models to predict changes in the GWL of an aquifer in eastern Rwanda. The KNN-RF model is more accurate than other models, as they determined from their research. They asserted that planning and managing GWL resources can benefit from the KNN-RF approach (Kombo et al., 2020). Kumar et al. (2020) predicted GWL using a DL model alongside extreme learning machine (ELM) and Gaussian process regression (GPR) models, in the Konan basin, Japan. They assessed the DL model's accuracy, which showed excellent agreement during validation (RMSE = 0.08, $r = 0.95$, NSE = 0.87). Re-validation at different stations demonstrated its robustness and generalization capabilities, making it a reliable tool for predicting GWL and optimizing resource allocation in groundwater systems (Kumar et al., 2020). Sharafati et al. (2020) employed gradient boosting regression (GBR) to predict monthly GWL in the Rafsanjan aquifer, Iran, using various input variables, including satellite data and pumping rates. They used the gamma test (GT) for feature selection and assessed performance using error metrics. The GBR yielded high predictive accuracy, especially with the gravity recovery and climate experiment (GRACE) dataset (Sharafati et al., 2020). Correlation analysis showed coefficient of determination values ranging from 0.66 to 0.94 for different lead times, with better accuracy in regions with higher water depth and pumping rates. The study offers valuable insights for water resource planning based on accurate modeling (Sharafati et al., 2020). Banadkooki et al. (2020) aimed to predict GWL using precipitation and temperature data with various temporal delays. They employed the radial basis function-whale algorithm (RBF-WA), multilayer perceptron (MLP-WA), and genetic programming (GP) to build hybrid ANN models. Results showed that the MLP-WA model outperformed others

when using temperature data with delays of 3, 6, and 9 months. Combining precipitation and temperature data with these delays yielded the best results (Banadkooki et al., 2020).

Osman et al. (2021) used three Xgboost models, an ANN, and vector regression to predict the GWL in Selangor, Malaysia. This study used 11 months from October 2017 to July 2018 to collect data for the models, including rainfall, temperature, previous day's water level, and evaporation. The study's conclusions showed that the Xgboost model produces more accurate prediction results (Osman et al., 2021). Malakar et al. (2021) predicted future GWL trends in India using GRACE-derived GWS, WaterGap model-based GWR, and GWW. Their LSTM model outperformed FNN and RNN, showing >84% of wells with $r > 0.6$ and RMSE < 0.7. They anticipate declining GWL trends in northwest, north-central, and south India, which could impact water supply and crop production for 1.3 billion people (Malakar et al., 2021). Afan et al. (2021) employed deep learning (DL) and ensemble deep learning (EDL) techniques to predict GWL in Malaysia. Their results revealed that EDL outperformed DL in estimating GWL, except for the Paya Indah Wetland. Additionally, EDL demonstrated superior performance in predicting daily GWL across all stations, reducing errors and providing precise results within a shorter time lag. Overall, they revealed that the EDL model has the potential to contribute to the sustainable management of GWL in Malaysia (Afan et al., 2021). Khan et al. (2023) reviewed GWL prediction models comprehensively. They examined 109 research articles and concluded that ML and deep learning approaches are efficient for modeling GWL. They also suggested future research directions to enhance prediction accuracy and understanding in this field (Khan et al., 2023). Dehghani and Torabi Poudeh, (2022) predicted GWL in southwest Iran by employing several meta-heuristic algorithms, including Feed-forward neural network (FNN) and automated item generation (AIG) models. Utilizing data on monthly rainfall, temperature, and water table height from the Lorestan Regional Water Corporation spanning 2008 to 2018, their study demonstrated the superior accuracy of the ANN-AIG hybrid model compared to other methods (Dehghani and Torabi Poudeh, 2022). Mohammed et al. (2023) combined a numerical model called GMS with methods like GA-ANN, GA-ICA, extreme learning machine (ELM), and ORELM in order to predict the GWL using piezometric data and rainfall information. The results of this investigation showed that, compared to other methods, the ORELM method accurately predicts the level of GWL (Mohammed et al., 2023). Table 1 shows the research work for the literature reviews used to predict GWL.

So far, no systematic study has been conducted to estimate the GWL in Izeh City, which is located in the Khuzestan province of Iran. Given that the region's primary occupation is agriculture and the prevalent use of GWL for domestic, agricultural, and industrial purposes, accurate GWL prediction can significantly impact water supply and crop production in this area.

2 Methodology

The diagram depicted in Figure 1 illustrates the prediction procedure for GWL employing both traditional and deep ML algorithms, including DT, RF, SVM, CNN, GAN, and RNN. The

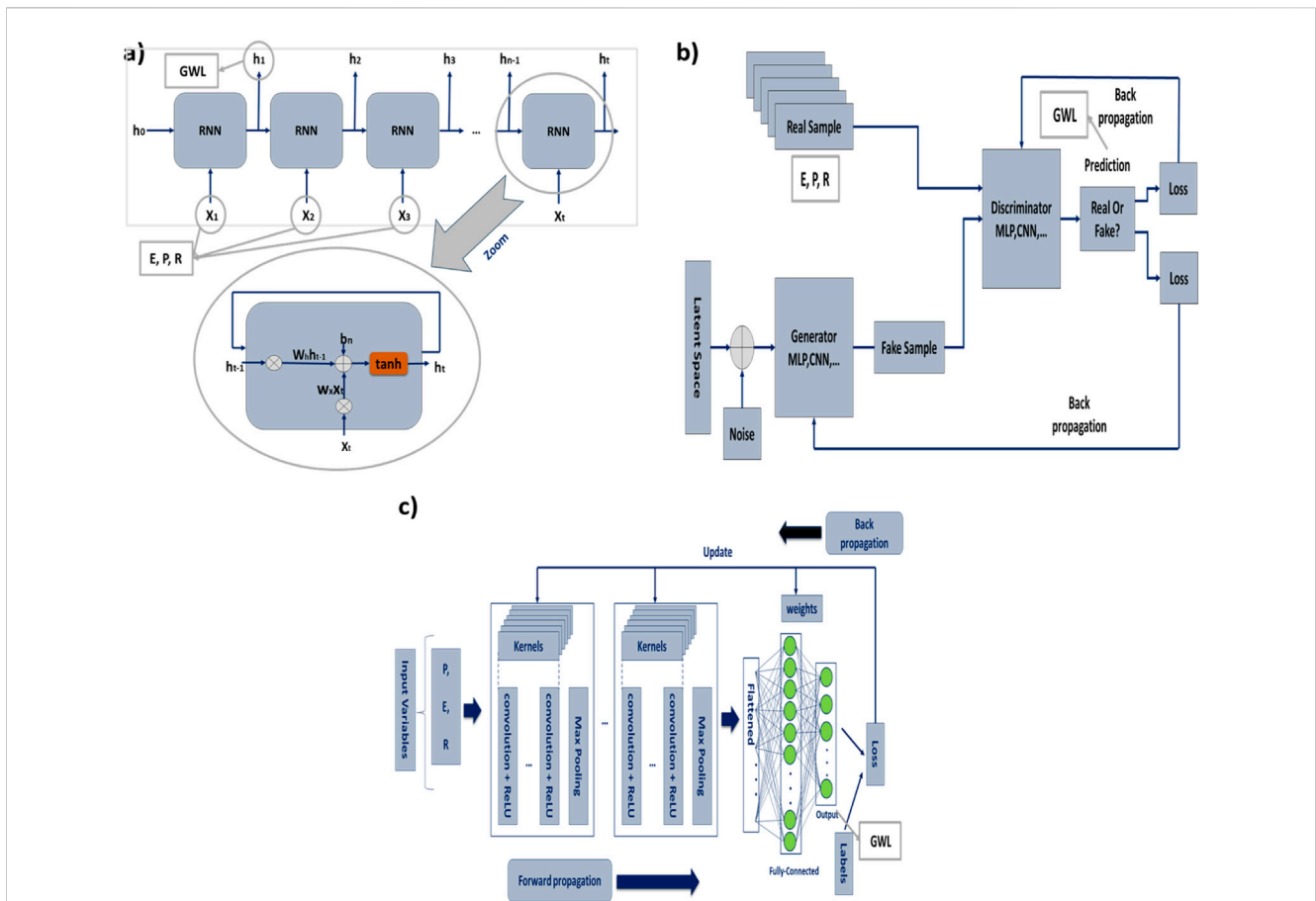


FIGURE 2 Illustration of the (A) chain of RNN network, (B) GAN network, (C) CNN algorithm for prediction of GWL.

TABLE 2 The hyperparameters for RNN algorithm.

Parameters	Values
Chaos	1.5
Time constant for model unit	0.3
Learning rate	1.0
Time constant of filtered white noise inputs	0.1
White noise input weight	0.001
Number of training iterations	100
Data time step size	0.01
Model RNN integration step size	0.001

initial step of executing this methodology involves the collection of data from Iran’s study area. Subsequently, the dataset undergoes sorting and preprocessing stages, which encompass the removal of outliers and duplicate data points. Following this, the data points are normalized using Eq. (1).

$$\omega_i^l = \left(\frac{\omega_i^l - \omega_{min}^l}{\omega_{max}^l - \omega_{min}^l} \right) * 2 - 1 \tag{1}$$

Finally, the dataset is randomly partitioned into training, testing, and validation sets. To compare traditional and deep ML, various

metrics, such as RMSE and R-Square, are computed for each algorithm. Sophistic ML models like CNN, GAN, and RNN are developed using preprocessed data. Ultimately, the models’ performances are juxtaposed, leading to the selection of CNN as the optimal approach for predicting GWL.

2.1 Traditional machine learning

2.1.1 Decision tree (DT)

The DT is a widely used supervised ML algorithm that is particularly valuable for classification and prediction tasks by dividing data into sub-trees and branching out further (Kotsiantis, 2013). In this algorithm, the input variables (R, P, and E) are considered trees, and the control parameters related to the RF algorithm are considered nodes between the trees. Finally, the final decision is known as the GWL prediction. This study employed a regression decision tree model with specified parameters. The maximum depth of the tree was set to 100, indicating the maximum number of levels in the tree structure. The criterion for measuring the quality of a split was chosen as “Gini,” which typically assesses impurity for classification tasks, although it is worth noting that for regression tasks, other criteria like “mse” (Mean Squared Error) might be more common. The splitter strategy was set to “best,” meaning the algorithm considers

TABLE 3 The hyperparameters for the GAN algorithm.

Parameters	Values
Generator time	1.1
Bot filter quantile	0.0001
Top filter quantile	0.99
Loss	RMSE
Maximum depth	2
Maximum bin	100
Learning rate	0.001
Random state	yes
Estimators	100
Batch size	500
Patience	25

all possible splits and selects the one that optimally reduces impurity or minimizes the mean squared error.

2.1.2 Random forest (RF)

The RF algorithm amalgamates the predictions stemming from all constituent trees within the forest, averaging them to yield a prediction that is not only more robust but also more accurate (Gomes et al., 2017). This ensemble approach effectively counteracts the influence of individual trees that might have generated erroneous predictions or excessively adhered to the training data's idiosyncrasies. In this algorithm (RF) context, the input and output variables (R, P, E, and GWL) are metaphorically conceptualized as trees. The aggregate decisions and the ultimate amalgamated tree are denoted as the GWL outcomes upon culmination. This study employed a regression random forest model with specific parameter settings. The maximum depth of the trees in the forest was set to 100, indicating the maximum number of levels in each decision tree. The random state was fixed at 0, ensuring reproducibility by keeping the randomness constant. The number of decision trees in the forest was set to 0, which typically means an unrestricted growth of trees until the specified maximum depth is reached. The objective function used for training the model was the Mean Squared Error (MSE), a measure that quantifies the average squared difference between the predicted and actual values, guiding the optimization process toward minimizing prediction errors.

2.1.3 Support vector machines (SVM)

The versatility of SVM is evident in its utilization for both classification and regression tasks, mirroring the functionalities of DT and RF algorithms (Wang et al., 2022). The algorithm diligently endeavors to expand these margins to their fullest potential, effectively delving into the essence of generalized error learning theory and striving to minimize errors to the greatest extent possible (Kecman, 2001). This endeavor aligns with SVM's overarching objective of achieving optimal separation between distinct classes or the prediction of accurate numerical values in regression scenarios (Ozer et al., 2020). In this algorithm, the input

TABLE 4 The hyperparameters for the CNN algorithm.

Parameters	Values
Input layer	37
CONV layer 1(f = 3, s = 1)	74
POOL layer 1	24
CONV layer 2(f = 3, s = 1)	28
POOL layer 2	16
Fully connected layer 1	14
Fully connected layer 2	8
Softmax	4
Kernel size	3
Stride size	1

variables (R, P, and E) are the objective parameters discussed in this article, while the output variable (GWL) is the predictive parameter. In this study, a prediction model was developed with specific hyperparameters: a batch size of 100, determining the number of training samples processed in a single iteration; a regularization parameter (C), which helps control overfitting by penalizing significant coefficients in the model, set to 0.1; and the utilization of a polynomial kernel.

2.2 Deep machine learning

2.2.1 Recurrent neural network (RNN)

An RNN is a specialized neural network for handling sequential and time-series data, particularly suited for prediction GWL based on input parameters P, R, and E (Panahi et al., 2020). Unlike multilayer perceptron (MLP) and CNN architectures, RNNs emphasize time considerations. While feed-forward networks like CNNs are common, RNNs incorporate a feedback loop, enabling them to retain prior inputs and process input sequences, preserving information across moments (Kanjo et al., 2019; Garbin et al., 2020). This characteristic ensures historical data's retention within the network. Figure 2A presents an RNN cell example (Han et al., 2021).

An RNN consists of a hidden state memory input ('h') and a primary input 'x' (R, E, and P) (Ming et al., 2017). Processing occurs through layers 'wh' and 'wx' for 'h' and 'x', respectively. 'ht-1' and 'xt' is multiplied by 'wh' and 'wx' weight matrices (Mirjalari et al., 2020) summed as per Eq. (2), and activated by functions like tanh, sigmoid, relu, etc. (Giordano et al., 2019) to yield 'ht.' See Figure 2A for the RNN architecture.

$$h_t = f(w_h h_{t-1} + w_x x_t + b_h) \quad (2)$$

The output above corresponds to the next hidden state (h_t) and the output of the RNN at time t . In Figure 2A X (1) serves as the input sequence; $h(0)$ and X (1) combine for the subsequent stage. Outputs $h(1)$ and X (2) in the following stage form input. During training, previous inputs are remembered (Shi et al., 2017). Unfolding the RNN over time creates a network chain. Hyperparameters are detailed in Table 2. In the realm of predicting GWL using an RNN algorithm, controlling chaos is

TABLE 5 Report of input/output variables in order to predict GWL for the data related to Izeh City of Khuzestan province of Iran.

Variable	Groundwater extraction rate	Groundwater recharge		Groundwater level
		Rainfall rate	River flow rate	
Abbreviation	E	R	P	GWL
Unit	m ³ /day	mm ³ /day	m ³ /day	m
Ave	5457.65	9.99	2,861.70	142.19
Std. Dev	253.18	11.25	221.91	6.11
Var	64070.96	126.47	49222.68	37.30
Min	5014.59	0.00	2,340.57	135.17
Max	5907.05	34.42	3359.47	157.69
Skew	0.03	0.58	-0.02	1.12
Kurt	-1.21	-1.21	-0.69	0.18

important for stability. Adjusting the time constant for model units aids in capturing the system's dynamics while optimizing the learning rate to fine-tune the model's responsiveness. The time constant of filtered white noise inputs and the weight assigned to white noise inputs influence noise incorporation, demanding careful calibration. Iterating the training process and modifying the data time step size ensures model accuracy with evolving data patterns. Furthermore, the RNN integration step size impacts temporal resolution, necessitating strategic adjustments to balance precision and computational efficiency in predicting GWL.

2.2.2 Generative adversarial networks (GAN)

The GANs, comprising a generator and a discriminator, identify data patterns autonomously, engaging in a competition to evolve the dataset (Shi et al., 2017). Figure 2B shows a GAN network.

The GANs consist of two neural networks: a generator $G(x)$ and a discriminator $D(x)$. The generator produces synthetic samples to increase the likelihood of fooling the discriminator (Dong and Lin, 2019). It takes noise vectors and generates fake data. Real and fake data are then fed to the discriminator, which categorizes them (Li et al., 2019). The model is trained by calculating the loss at the discriminator's end and adjusting parameters via backpropagation (Alarsan and Younes, 2021). The GAN training process involves selecting real data (X), passing it through the generator and applying sigmoid activation, creating noise data (Z), generating samples ($G(Z)$), evaluating loss, backpropagating to update discriminator weights, using generator output to update its weights, and iterating until optimal weights are achieved for both networks.

The discriminator loss function assesses D 's prediction on real/fake data, calculated from errors made. Errors backpropagate to update parameters (Azari et al., 2022). It comprises terms for real (x) and fake ($G(z)$) inputs, with the real input loss term defined as expressed in Eq. (3). The second term is for fake input ($G(z)$) as expressed in Eq. (4).

$$l_{d_1} = \log \sigma(D(x)) \quad (3)$$

$$l_{d_2} = \log(1 - \sigma(D(G(z)))) \quad (4)$$

In the equation, σ is the sigmoid function with an output range of 0–1. An output near 1 implies accurate real data recognition by D , resulting in minimal loss (Szandała, 2021).

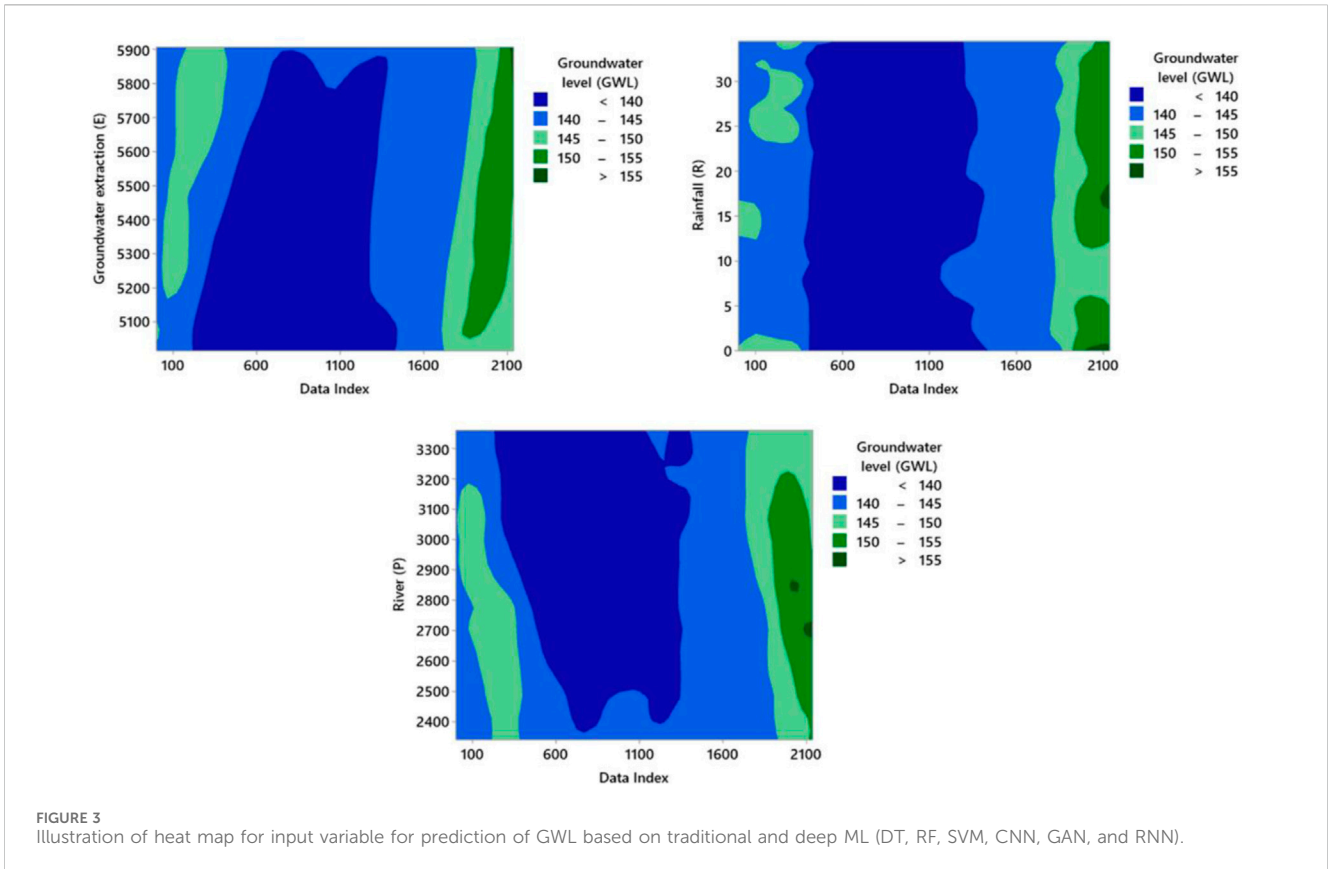
The two-loss terms are computed and summed for the overall discriminator network loss. The GAN hyperparameters, which are pivotal for performance, are detailed in Table 3. Due to GAN-type variance, tuning is essential. The generator time impacts training duration and data quality; the lower filter quantile prevents biased results, and the top filter quantile maintains alignment. The loss function improves GAN via data distinctions, and the maximum depth affects complexity and overfitting. The maximum bin and learning rate control convergence, ensuring reproducibility through a random state. Estimators boost diversity, batch size influences stability, and patience counters overfitting. Control parameters are fixed through careful calibration and iterative experimentation to optimize performance for the prediction of GWL.

2.2.3 Convolutional neural network (CNN)

The CNN emulates the visual cortex with neurons, weights, and biases. It comprises convolutional, pooling, and fully connected layers (Azizah et al., 2017). Notably, the convolutional layer employs operations, while the fully connected layer maps characteristics to output. The CNNs maintain input structure, highlighting data relationships (Yamashita et al., 2018). Training entails optimizing parameters via backpropagation and gradient descent. Figure 2C shows the structure of the CNN algorithm.

The main kernel of the CNN is the convolutional layer, which has assigned most of the computations to the CNN (Wang et al., 2017). Each convolutional layer in the CNN consists of a set of filters, and the output is created from the convolution between the filters and the input layer (O'Shea and Nash, 2015). The output of the convolutional layer is called a feature map.

In CNNs, the convolution operator slides a kernel over the input, multiplying its values with input values, creating a feature map (Wang et al., 2021). Kernel count and size dictate operation complexity, often 3×3 , 5×5 , or 7×7 . The number determines the output feature map depth. Padding maintains input size. The CNN hyperparameters are in Table 4. Each control parameter serves a specific function in the CNN algorithm for predicting GWL. The input layer processes the initial data, the CONV layer extracts features through convolution, the POOL layer reduces spatial dimensions, and the Fully Connected layer combines features for



classification. Softmax provides probability scores. Kernel size determines feature extraction scope, and Stride size controls filter movement. Fixing parameters involves tuning through iterative training and adjusting based on model performance and validation results.

2.3 Spearman’s and Pearson’s correlation and error metrics

One of the best methods for determining the relative importance of input-independent variables compared to output-dependent variables (GWL) is to use the Pearson’s coefficient (R) method. This coefficient expresses a correlation between -1 and $+1$. Based on this coefficient, a value of $+1$ has the most significant positive impact, and a value of -1 has the most significant absolute impact, while a zero value means there is no linear relationship between two variables. Also, this parameter shows that it has no effect. The Pearson’s correlation is shown in Eq. (5) (De Winter et al., 2016).

$$Z = \frac{\sum_{i=1}^n (P_i - \bar{P})(K_i - \bar{K})}{\sqrt{\sum_{i=1}^n (P_i - \bar{P})^2} \sqrt{\sum_{i=1}^n (K_i - \bar{K})^2}} \quad (5)$$

Spearman’s coefficient (ρ) is one of the coefficients of the input data set compared to the output for the input variables compared to the output variables. Data can be ranked using this parameter. This equation is in the form of Eq. (6) (Alsaqr, 2021).

$$\rho = \frac{\sum_{i=1}^n (P_i - \bar{P})(K_i - \bar{K})}{\sqrt{\sum_{i=1}^n (P_i - \bar{P})^2} \sqrt{\sum_{i=1}^n (K_i - \bar{K})^2}} \quad (6)$$

In order to compare and measure the comparison, the equations and statistical errors reported in Equations (7–9) are used.

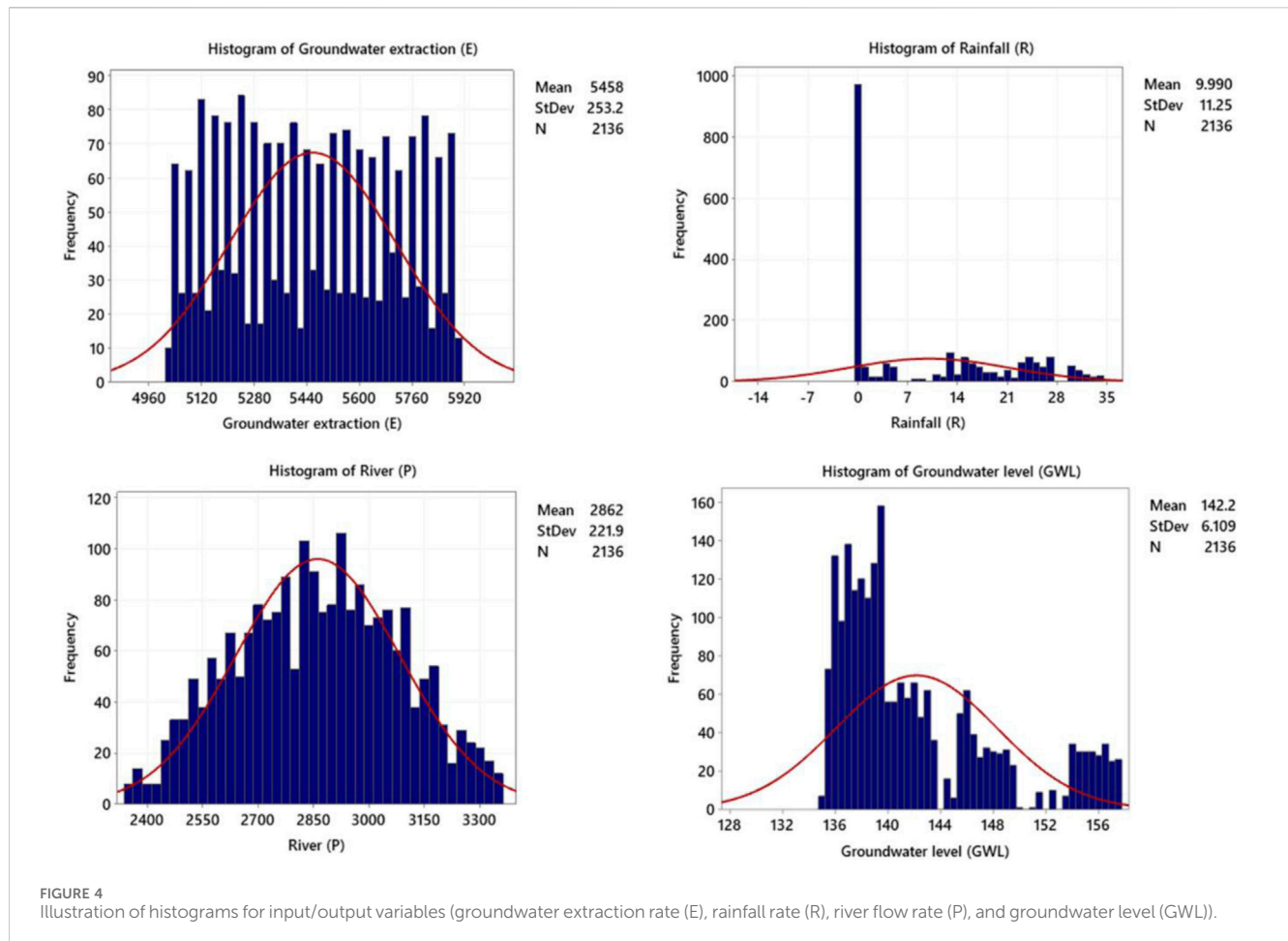
$$STD = \sqrt{\frac{\sum_{i=1}^n \left(\left(\frac{GWL_{(Meas)} - GWL_{(Pre)}}{GWL_{(Meas)}} \times 100 \right)_i - \left(\frac{1}{n} \sum_{i=1}^n (GWL_{Meas,i} - GWL_{Pre,i}) \right) \right)^2}{n - 1}} \quad (7)$$

$$RMSE = \sqrt{\frac{1}{n} \sum_{i=1}^n (GWL_{Meas,i} - GWL_{Pred,i})^2} \quad (8)$$

$$R^2 = 1 - \frac{\sum_{i=1}^n (GWL_{Meas,i} - GWL_{Pre,i})^2}{\sum_{i=1}^n \left(GWL_{Pre,i} - \frac{\sum_{i=1}^n GWL_{Meas,i}}{n} \right)^2} \quad (9)$$

3 Data gathering and data distribution

River water imports, precipitation, and the negative parameter of GWL withdrawal are among the positive parameters for GWL (Machiwal and Singh, 2015; Zhang et al., 2019). To predict this essential and vital parameter for human society, 2136-point data collected from 2018 to 2022 employing various methods, such as a water level sensor for groundwater level, a flow meter for groundwater extraction rate, a rain gauge for rainfall rate, and a stream gauge for river flow rate with 3 km distance, was gathered



from Izeh City in the Khuzestan province of Iran for this article. Both Izeh City's hydrology influences hydrology in Izeh City is influenced by human activities and seasonal changes (Kalantari et al., 2009; Hoseini, 2022). Human activities such as agriculture and industrialization significantly impact the region's hydrological system (Nassery et al., 2009; Rashidi and Hosseinzadeh, 2019). Agricultural practices, particularly irrigation, heavily rely on E, which can lower the water level and alter the natural balance (Jafari et al., 2015; Neissi et al., 2020). Industrial activities and urbanization contribute to changes in surface runoff patterns and can introduce pollutants into water sources (Rashidi and Hosseinzadeh, 2019; Ziyari and Latifi, 2022). Additionally, seasonal variations play a crucial role in the hydrological cycle of Izeh City (Bakhtiari et al., 2021). During the rainy season, increased precipitation and runoff lead to rising GWL, while dry seasons result in decreased groundwater recharge due to higher evaporation rates (Kalantari et al., 2009). Understanding the intricate relationship between human activities, seasonal changes, and hydrology is vital for sustainable water resource management in Iran's Izeh City of Khuzestan province (e.g., Nassery et al., 2009; Mahdavi et al., 2021).

In order to build a hybrid model of AI, 70% of the data is used for training, 15% for testing, and 15% for validation. The use of data to build the model is random. The statistical information related to the data used in this article is reported in Table 5. Based on this table, the range and values of statistical parameters are reported.

A heat map is used in order to distribute the data. As shown in Figure 3, 400 data points of the E are in the range of $145 < \text{GWL} < 150$, 1,300 data points of the E are in the range of $140 < \text{GWL} < 145$, and 436 data points of the E are in the range of $\text{GWL} < 140$.

As shown in that figure, 300 data points of the R are in the range of $145 < \text{GWL} < 150$, 1,100 data points of the R are in the range of $140 < \text{GWL} < 145$, and 736 data points of the R are in the range of $\text{GWL} < 140$.

Also, 300 data points of the P are in the range of $145 < \text{GWL} < 150$, 1,236 data points of the P are in the range of $140 < \text{GWL} < 145$, and 600 data points of the P are in the range of $\text{GWL} < 140$.

To present the Mean and StDev values, we have included the data distribution and data values in Figure 4. As depicted in Figure 4, the histograms visually represent the input/output variables, including E, R, P, and GWL. The distribution of the recorded values is displayed in the histogram for E, which also reveals the frequency of various extraction levels. Similarly, the histogram for R presents the distribution of R values, allowing us to observe the frequency of different precipitation amounts. The histogram for P displays the distribution of P data, providing an overview of the frequency of P measurements. Lastly, the histogram for GWL illustrates the distribution of measured values, giving us an understanding of the frequency of different water level readings.

TABLE 6 Statistical reports related to train, test, validation, and total results were used to predict GWL based on traditional and deep ML (DT, RF, SVM, CNN, GAN, and RNN).

Split dataset	Model	STD	RMSE	R ²
Train	CNN	0.0506	0.0507	0.9968
	RNN	0.1372	0.1375	0.9887
	GAN	0.3854	0.3857	0.9559
	DT	1.8314	1.8517	0.8388
	RF	2.4736	2.4479	0.7632
	SVM	2.6471	2.6532	0.7234
Test	CNN	0.0561	0.0561	0.9951
	RNN	0.2004	0.2004	0.9845
	GAN	0.4085	0.4086	0.9403
	DT	2.0513	2.6517	0.8532
	RF	2.8881	2.8884	0.7715
	SVM	3.0615	3.0615	0.7417
Validation	CNN	0.0593	0.0594	0.9926
	RNN	0.2135	0.2197	0.9799
	GAN	0.4130	0.4130	0.9394
	DT	2.0009	2.0010	0.8523
	RF	2.7894	2.8963	0.7709
	SVM	3.0043	3.0017	0.7398
Total	CNN	0.0558	0.0558	0.9948
	RNN	0.2026	0.2025	0.9844
	GAN	0.4086	0.4084	0.9452
	DT	1.9612	2.1681	0.8481
	RF	2.7170	2.7442	0.7685
	SVM	2.9043	2.9055	0.7350

By examining this histogram, we can gain insights into the variability and distribution of GWL, which are crucial for assessing groundwater resources and potential fluctuations (e.g., Kumar and Ahmed, 2003; Ahmadi and Sedghamiz, 2007; Dash et al., 2010).

4 Discussion of results

In order to predict this critical parameter, DT, RF, SVM, CNN, GAN, and RNN traditional and deep ML algorithms have been used. The reports related to the results of training, testing, validation, and total data are given in Table 6.

This article uses traditional and deep ML (DT, RF, SVM, CNN, GAN, and RNN) methods to predict GWL. The statistical parameters R², STD, and RMSE are used to evaluate the delivered models in Table 6. After checking the results from Table 6, it is clear that the reports of the CNN model are better than those of the RNN and GAN models. Based on the results

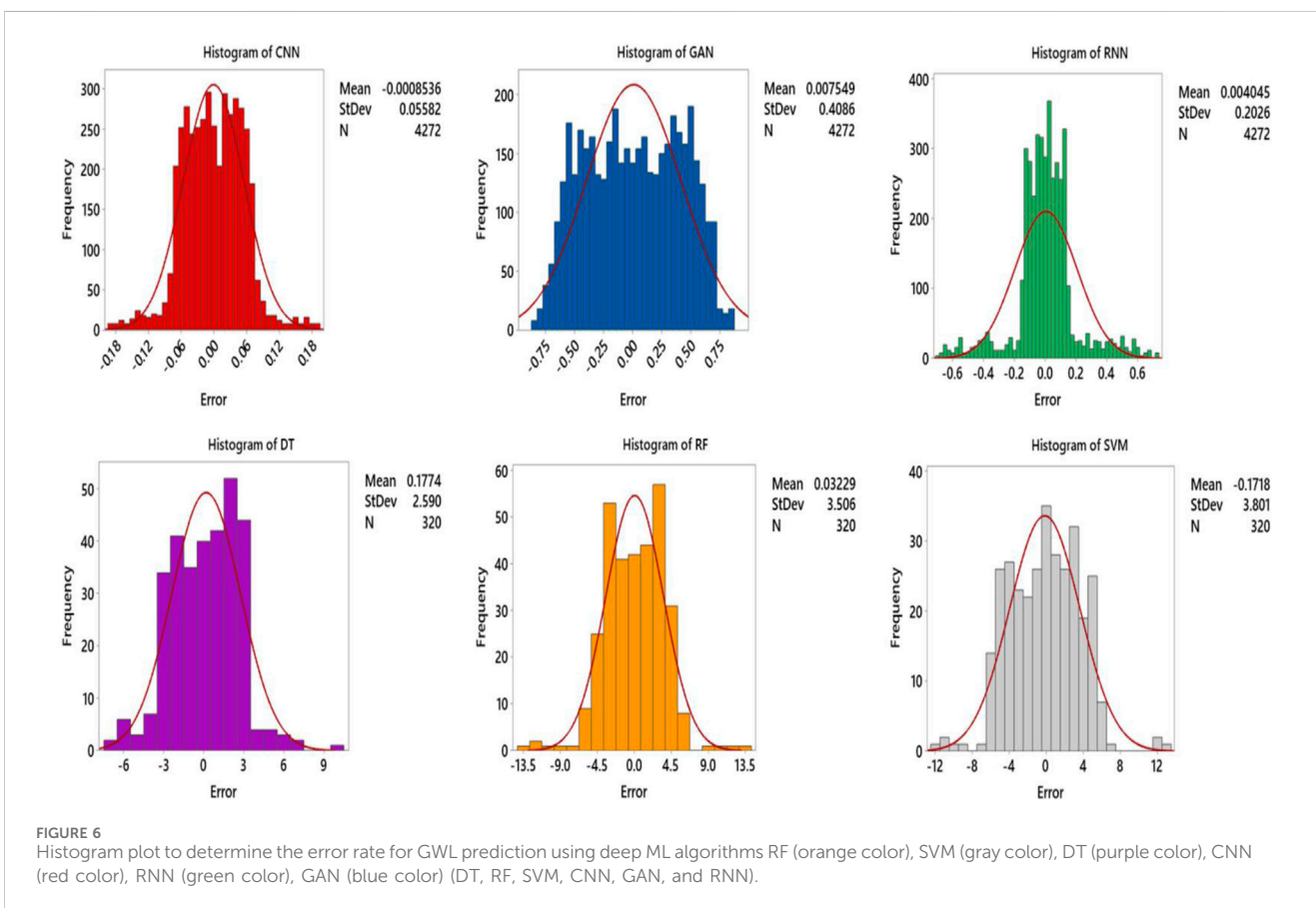
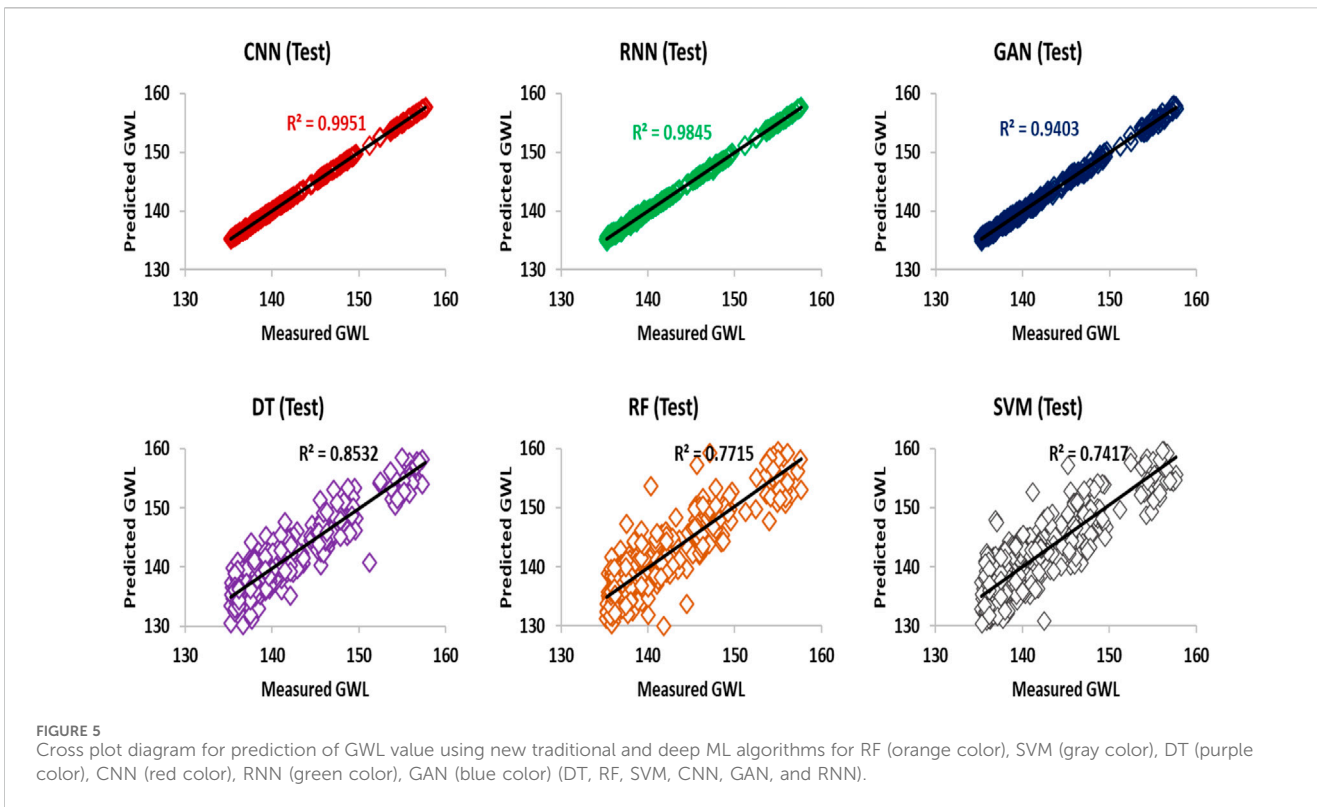
shown, it is determined that the values of RMSE and R² for train, test, validation, and total data are [0.0507, 0.0561, 0.0594, 0.0558] and [0.9968, 0.9951, 0.9926, 0.9948], respectively.

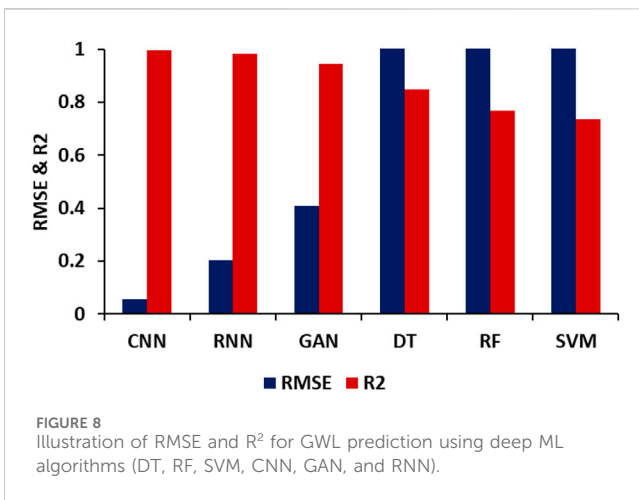
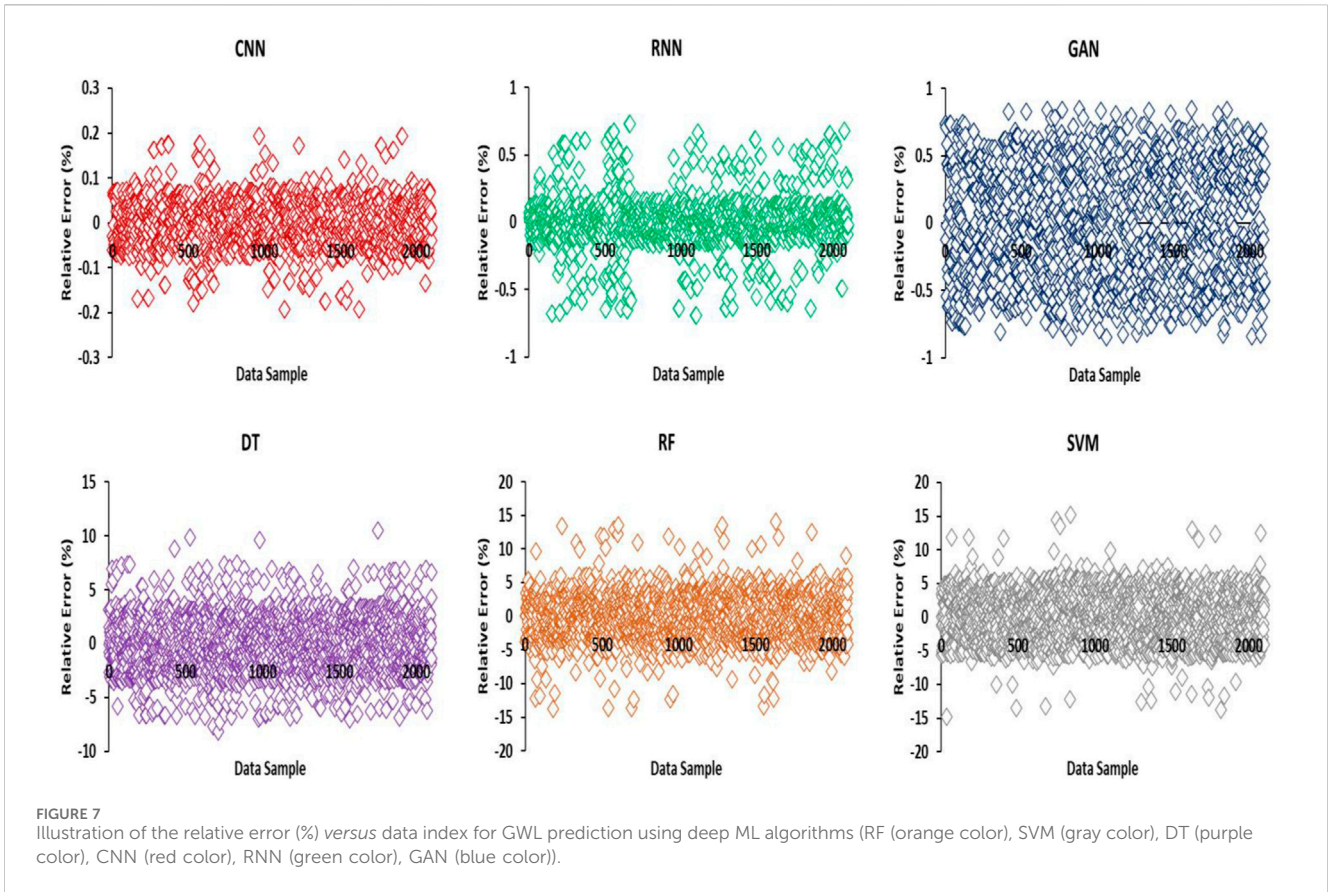
Based on Figure 5, which shows the cross plot between the measured data points and the predicted data, the best AI model for regression can be determined from among the models provided. This figure gives six traditional and deep ML models (DT, RF, SVM, CNN, GAN, and RNN). Based on this figure, a good comparison can be made between the models based on R². Based on the results presented visually for the whole dataset, it is clear that the RNN algorithm has a higher accuracy than the other algorithms. Based on the results shown, it is clear that the accuracy of these algorithms is SVM < RF < DT < GAN < RNN < CNN.

Figure 6 shows the histogram of the GWL prediction error for three newly developed deep ML algorithms. As shown in the histogram diagram, GWL prediction errors are symmetrically distributed at the zero point, and for the CNN algorithm, this distribution is normal. Its statistical error distribution is either positively or negatively distributed.

Based on the data presented in Figure 7, which illustrates the relative error (%) versus data index for GWL prediction using deep ML algorithms RNN, CNN, and GAN, we can analyze the error ranges associated with each algorithm (e.g., Yoon et al., 2011; Banadkooki et al., 2020; Di Nunno and Granata, 2020; Azari et al., 2021). The figure provides valuable insights into the accuracy of the DT, RF, SVM, CNN, GAN, and RNN algorithms by depicting their respective relative error (%) ranges. Upon examining Figure 7, we observe that the error range for the CNN algorithm falls between -0.192 and 0.194. In contrast, the RNN algorithm exhibits an error range of -0.693 to 0.729, while the GAN algorithm spans from -0.850 to 0.850, the DT algorithm exhibits an error range of -8.1936 to 10.4948, and the RF algorithm exhibits an error range of -13.7735 to 14.085. These error ranges show the magnitude and direction of the relative errors between the predicted and actual GWL values (e.g., Yoon et al., 2011; Marchant et al., 2016). Based on this information, it is concluded that the CNN algorithm outperforms the RNN and GAN algorithms in terms of accuracy. The GWL predictions made by the CNN algorithm exhibit a smaller relative error (%) when compared to the RNN, GAN, DT, RF, and SVM algorithms. Therefore, a comparison of these algorithms reveals that the accuracy ranking is as follows: CNN > RNN > GAN > DT > RF > SVM.

According to the graphical data in Figure 8 and Table 6, which show the RMSE and R² for GWL prediction utilizing deep ML algorithms (DT, RF, SVM, CNN, GAN, and RNN), the performance accuracy of RMSE and R² yields contrasting results. In other words, as the R² value increases, the corresponding RMSE value decreases. Furthermore, this figure effectively demonstrates the performance accuracy of the algorithms employed for GWL prediction, with the ranking as follows: CNN > RNN > GAN > DT > RF > SVM. Figure 8 provides valuable insights into the relationship between RMSE and R² in the context of GWL prediction. As the R² value increases, it indicates a stronger correlation between the predicted and actual GWL values (e.g., Sakaguchi and Berge, 1998; Seifi et al., 2020; Wu et al., 2023). Consequently, the RMSE value decreases, signifying a smaller average error in the prediction (e.g., Mukherjee and Ramachandran, 2018; Yosefvand and Shabanlou, 2020; Iqbal





et al., 2021; Lin et al., 2022; Samantaray et al., 2022). The figure reinforces the conclusion that the CNN algorithm outperforms the RNN and GAN algorithms in terms of accuracy for GWL prediction. The higher R² and lower RMSE values associated with CNN demonstrate its superior performance compared to the other algorithms. Therefore, the comparative analysis suggests the following accuracy ranking: CNN > RNN > GAN > DT > RF > SVM.

A comparison of Pearson and Spearman correlation coefficients based on Figure 9 can provide insight into the relationship between

input variables and GWL (e.g., Hauke and Kossowski, 2011; Worsa-Kozak et al., 2020; Balacco et al., 2022). The observed negative correlation between groundwater recharge (R and P) and GWL indicates that these input factors yield a negative influence when incorporated into the linear relationship governing GWL or when included in the proportion it affects. In contrast, the observed positive correlation between E and GWL indicates that E has a positive power or direct proportionality when placed in the physical linear relationship of GWL (e.g., Hauke and Kossowski, 2011; Mukherjee and Ramachandran, 2018). The E involves drawing water from underground aquifers for purposes like irrigation, industry, and domestic use (Foster and Chilton, 2003; Worsa-Kozak et al., 2020). This often leads to declining GWL as extraction outpaces natural replenishment from R and infiltration, creating a positive correlation between E and GWL reduction.

In contrast, P can exhibit a negative correlation with GWL due to stream-aquifer interaction. Elevated GWL can feed P, bolstering their flow, while low GWL prompts P to recharge adjacent aquifers by seeping water into the ground, establishing a dynamic that yields a negative correlation between P and GWL. Given that the Pearson value for R is approximately -0.00357 and close to zero, it can be assumed that this parameter has little effect on GWL. The use of both Pearson and Spearman correlation methods provides a robust analysis of the data, and the results can be used to develop GWL prediction models based on the input variables (Hauke and Kossowski, 2011; Worsa-Kozak et al., 2020). Expressing the relationships between input variables and GWL in Eq. (10)

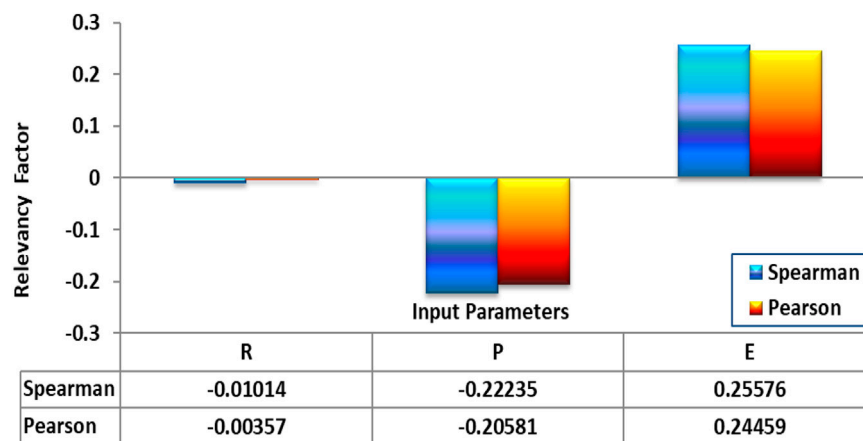


FIGURE 9
Correlation between input and output parameters for Pearson and Spearman equations to predict GWL.

allows quantitative data analysis and facilitates comparison with other studies.

$$GWL = \alpha (E) \quad \text{and} \quad GWL = \alpha \frac{1}{(P, R)} \quad (10)$$

The analysis of the Spearman and Pearson correlation coefficient values indicates that variables P and E have a stronger influence on GWL than variable R. This suggests that E and P flow are more significant factors affecting GWL than R (e.g., Kim et al., 2016; Csáfordi et al., 2017). However, it is important to note that the relative importance of these variables may vary depending on the specific site conditions and hydrological characteristics. The relative contributions of these variables to GWL can be determined with the aid of additional analysis, such as regression modeling, which can also offer insights into the underlying mechanisms causing the observed correlations (Hauke and Kossowski, 2011). The interpretation of the correlation coefficients should also consider the statistical significance of the results as well as the potential for confounding variables or measurement error (Mukherjee and Ramachandran, 2018; Iqbal et al., 2021).

Deep learning's outstanding capabilities include forecasting crucial GWL characteristics (Sit et al., 2020; Afan et al., 2021; Wunsch et al., 2021). By employing powerful algorithms, these predictions can ensure accurate estimations, meet the water supply needs of the people in the Izeh area, and enhance their quality of life. The AI, including deep learning, has demonstrated its value in predicting GWL parameters. Leveraging these sophisticated algorithms, we can achieve precise predictions, thereby effectively addressing the water supply requirements of the community in Izeh and safeguarding their wellbeing.

5 Limitation

The limitations of this article are the lack of access to additional information about water diversion, evaporation rate, and temperature data in the target area, especially Izeh City. It is recommended that other researchers consider the influence of

these parameters due to their considerable availability when predicting GWL. Including these parameters in the prediction model can provide a more accurate estimate of groundwater resources. This is particularly important because various factors, such as evaporation and temperature, affect GWL. Additionally, a similar article has not been published for Izeh City so far, and it has been somewhat challenging to provide data at this wide level.

Furthermore, it is essential to highlight that the effectiveness of CNN algorithms in predicting GWL is enhanced when a substantial number of input variables are employed. In this article, only three parameters were utilized as input variables, leading to the anticipation that augmenting the inputs will likely boost the accuracy of GWL predictions. Hence, it is recommended that researchers to incorporate a greater number of input variables to enhance the algorithm's accuracy.

6 Conclusion

An extensive 2,136 time series data points dataset has been collected from the Izeh City of Khuzestan province in Iran. The collected data was utilized using the DML technique to effectively predict the GWL in the proximate wellbore regions by means of three input variables: groundwater extraction rate (E), rainfall rate (R), and river flow rate (P). Through analysis, it has been discovered that deep machine learning (DML) algorithms, such as recurrent neural network (RNN), convolutional neural network (CNN), generative adversarial network (GAN), decision tree (DT), random forest (RF), and support vector machine (SVM), which are traditional and deep ML algorithms, can be employed to predict GWL with remarkable precision. Moreover, the correlation coefficient analyses of Pearson and Spearman revealed that the GWL is negatively and indirectly related to the input variables of groundwater recharge (R and P). However, the input variable "E" exhibits a positive correlation with GWL.

Furthermore, the Spearman and Pearson correlation coefficients ascertain that the input variables P and E have a more significant influence on GWL compared to variable R. Considering that the Pearson value for R is

approximately -0.00357 and close to zero, it can be inferred that this parameter has little effect on GWL. However, deep learning algorithms possess the capability to select impactful features and eliminate less influential ones. The level of GWL prediction accuracy achieved by the CNN model, applied to all data records in the comprehensive dataset, is impressive: $RMSE = 0.0558$ and $R^2 = 0.9948$. CNN, a cutting-edge deep ML algorithm that is a robust and efficacious ML tool for data point prediction processing, is applied in this study. Its capability to learn and detect patterns in vast datasets makes it an excellent choice for prediction data points with multiple input variables. Some of the advantages of using CNN over DT, RF, SVM, GAN, and RNN algorithms for the prediction of data points include robustness to noise and variability, scalability to handle extensive datasets with multiple input variables, parallelization for rapid processing speeds for real-time and near real-time applications, generalization to learn and identify patterns in data without explicit programming, and fewer outlier data predictions. This research can assist the residents of Izeh City in the Khuzestan province in conserving and managing their water resources and achieving increased crop productivity for the local economy. This approach can be applied to predict GWL in different parts of the world, and it can potentially improve water management in regions facing water scarcity due to global population growth.

Data availability statement

The data analyzed in this study is subject to the following licenses/restrictions: Data can be made available upon reasonable requests for academic purposes through the corresponding authors. Requests to access these datasets should be directed to hamzehghorbani68@yahoo.com.

References

- Afan, H. A., Ibrahim Ahmed Osman, A., Essam, Y., Ahmed, A. N., Huang, Y. F., Kisi, O., et al. (2021). Modeling the fluctuations of groundwater level by employing ensemble deep learning techniques. *Eng. Appl. Comput. Fluid Mech.* 15, 1420–1439. doi:10.1080/19942060.2021.1974093
- Ahmadi, S. H., and Sedghamiz, A. (2007). Geostatistical analysis of spatial and temporal variations of groundwater level. *Environ. Monit. Assess.* 129, 277–294. doi:10.1007/s10661-006-9361-z
- Alarsan, F. I., and Younes, M. (2021). Best selection of generative adversarial networks hyper-parameters using genetic algorithm. *SN Comput. Sci.* 2, 283. doi:10.1007/s42979-021-00689-3
- Alfarrah, N., and Walraevens, K. (2018). Groundwater overexploitation and seawater intrusion in coastal areas of arid and semi-arid regions. *Water* 10, 143. doi:10.3390/w10020143
- Alsaqr, A. M. (2021). Remarks on the use of Pearson's and Spearman's correlation coefficients in assessing relationships in ophthalmic data. *Afr. Vis. Eye Health* 80, 10. doi:10.4102/aveh.v80i1.612
- Azari, A., Zeynoddin, M., Ebtehaj, I., Sattar, A. M., Gharabaghi, B., and Bonakdari, H. (2021). Integrated preprocessing techniques with linear stochastic approaches in groundwater level forecasting. *Acta Geophys.* 69 (4), 1395–1411. doi:10.1007/s11600-021-00617-2
- Azari, M., Rafiei, H., and Akbarzadeh-T, M.-R. (2022). "Robust human movement prediction by completion-generative adversarial networks with huber loss," in 2022 29th National and 7th International Iranian Conference on Biomedical Engineering (ICBME), Tehran, Iran, Islamic Republic of, December, 2022, 198–204.
- Azizah, L. M. r., Umayah, S. F., Riyadi, S., Damarjati, C., and Utama, N. A. (2017). "Deep learning implementation using convolutional neural network in mangosteen

Author contributions

FF: Conceptualization, Formal Analysis, Funding acquisition, Methodology, Resources, Software, Validation, Visualization, Writing—original draft, Writing—review and editing. HG: Conceptualization, Data curation, Formal Analysis, Funding acquisition, Methodology, Software, Supervision, Validation, Visualization, Writing—original draft, Writing—review and editing. AR: Conceptualization, Funding acquisition, Methodology, Resources, Validation, Visualization, Writing—original draft, Writing—review and editing.

Funding

The author(s) declare that no financial support was received for the research, authorship, and/or publication of this article.

Conflict of interest

The authors declare that the research was conducted in the absence of any commercial or financial relationships that could be construed as a potential conflict of interest.

Publisher's note

All claims expressed in this article are solely those of the authors and do not necessarily represent those of their affiliated organizations, or those of the publisher, the editors and the reviewers. Any product that may be evaluated in this article, or claim that may be made by its manufacturer, is not guaranteed or endorsed by the publisher.

surface defect detection," in 2017 7th IEEE International Conference on Control System, Computing and Engineering (ICCSCE), Penang, Malaysia, November, 2017, 242–246.

Bakhtiari, M., Boloorani, A. D., Kakroodi, A. A., Rangzan, K., and Mousivand, A. (2021). Land degradation modeling of dust storm sources using MODIS and meteorological time series data. *J. Arid Environ.* 190, 104507. doi:10.1016/j.jaridenv.2021.104507

Balacco, G., Alfio, M. R., and Fidelibus, M. D. (2022). Groundwater drought analysis under data scarcity: the case of the Salento aquifer (Italy). *Sustainability* 14 (2), 707. doi:10.3390/su14020707

Banadkooki, F. B., Ehteram, M., Ahmed, A. N., Teo, F. Y., Fai, C. M., Afan, H. A., et al. (2020). Enhancement of groundwater-level prediction using an integrated machine learning model optimized by whale algorithm. *Nat. Resour. Res.* 29, 3233–3252. doi:10.1007/s11053-020-09634-2

Barzegar, R., Fijani, E., Moghaddam, A. A., and Tziritis, E. (2017). Forecasting of groundwater level fluctuations using ensemble hybrid multi-wavelet neural network-based models. *Sci. Total Environ.* 599, 20–31. doi:10.1016/j.scitotenv.2017.04.189

Bovolo, C. I., Parkin, G., and Sophocleous, M. (2009). Groundwater resources, climate and vulnerability. *Environ. Res. Lett.* 4, 035001. doi:10.1088/1748-9326/4/3/035001

Brunner, P., and Simmons, C. T. (2012). HydroGeoSphere: a fully integrated, physically based hydrological model. *Ground water* 50, 170–176. doi:10.1111/j.1745-6584.2011.00882.x

Csáfordi, P., Szabó, A., Balog, K., Gribovszki, Z., Bidló, A., and Tóth, T. (2017). Factors controlling the daily change in groundwater level during the growing season on the Great Hungarian Plain: a statistical approach. *Environ. Earth Sci.* 76, 1–16. doi:10.1007/s12665-017-7002-1

- Dash, J. P., Sarangi, A., and Singh, D. K. (2010). Spatial variability of groundwater depth and quality parameters in the national capital territory of Delhi. *Environ. Manag.* 45, 640–650. doi:10.1007/s00267-010-9436-z
- Dehghani, R., and Torabi Poudeh, H. (2022). Application of novel hybrid artificial intelligence algorithms to groundwater simulation. *Int. J. Environ. Sci. Technol.* 19, 4351–4368. doi:10.1007/s13762-021-03596-5
- De Winter, J. C. F., Gosling, S. D., and Potter, J. (2016). Comparing the Pearson and Spearman correlation coefficients across distributions and sample sizes: a tutorial using simulations and empirical data. *Psychol. methods* 21, 273–290. doi:10.1037/met0000079
- Di Nunno, F., and Granata, F. (2020). Groundwater level prediction in Apulia region (Southern Italy) using NARX neural network. *Environ. Res.* 190, 110062. doi:10.1016/j.envres.2020.110062
- Dong, J., and Lin, T. (2019). MarginGAN: adversarial training in semi-supervised learning. *Adv. neural Inf. Process. Syst.* 32.
- Eriksson, E. (1970). Groundwater time series: an exercise in stochastic hydrology. *Hydrology Res.* 1, 181–205. doi:10.2166/nh.1970.0012
- Foster, S. S. D., and Chilton, P. J. (2003). Groundwater: the processes and global significance of aquifer degradation. *Philosophical Trans. R. Soc. Lond. Ser. B Biol. Sci.* 358 (1440), 1957–1972. doi:10.1098/rstb.2003.1380
- Franses, P. H., and Van Dijk, D. (2000). *Non-linear time series models in empirical finance*. Cambridge, United Kingdom: Cambridge University Press.
- Garbin, C., Zhu, X., and Marques, O. (2020). Dropout vs. batch normalization: an empirical study of their impact to deep learning. *Multimedia Tools Appl.* 79, 12777–12815. doi:10.1007/s11042-019-08453-9
- Ghobadi, F., and Kang, D. (2023). Application of machine learning in water resources management: a systematic literature review. *Water* 15, 620. doi:10.3390/w15040620
- Giordano, M., Cristiano, G., Ishibashi, K., Ambrogio, S., Tsai, H., Burr, G. W., et al. (2019). Analog-to-digital conversion with reconfigurable function mapping for neural networks activation function acceleration. *IEEE J. Emerg. Sel. Top. Circuits Syst.* 9, 367–376. doi:10.1109/jetcas.2019.2911537
- Gomes, H. M., Bifet, A., Read, J., Barddal, J. P., Enembreck, F., Pfahringer, B., et al. (2016). Adaptive random forests for evolving data stream classification. *Mach. Learn.* 106, 1469–1495. doi:10.1007/s10994-017-5642-8
- Gong, Y., Zhang, Y., Lan, S., and Wang, H. (2016). A comparative study of artificial neural networks, support vector machines and adaptive neuro fuzzy inference system for forecasting groundwater levels near Lake Okeechobee, Florida. *Water Resour. Manag.* 30, 375–391. doi:10.1007/s11269-015-1167-8
- Han, T., Pang, J., and Tan, A. C. C. (2021). Remaining useful life prediction of bearing based on stacked autoencoder and recurrent neural network. *J. Manuf. Syst.* 61, 576–591. doi:10.1016/j.jmsy.2021.10.011
- Hauke, J., and Kosowski, T. (2011). Comparison of values of Pearson's and Spearman's correlation coefficient on the same sets of data. *Quaest. Geogr.* 30 (2), 87–93. doi:10.2478/v10117-011-0021-1
- Hay, J. E., and Mimura, N. (2005). Sea-level rise: implications for water resources management. *Mitig. Adapt. Strategies Glob. Change* 10, 717–737. doi:10.1007/s11027-005-7305-5
- Hoseini, Y. (2022). Evaluation of WMS model in basins without statistical data in southwestern Iran using Dicken's experimental method (case study: kuhgel Basin of Khuzestan Province). *Appl. Water Sci.* 12 (7), 162. doi:10.1007/s13201-022-01685-5
- Hughes, J. D., Russcher, M. J., Langevin, C. D., Morway, E. D., and McDonald, R. R. (2022). The MODFLOW Application Programming Interface for simulation control and software interoperability. *Environ. Model. Softw.* 148, 105257. doi:10.1016/j.envsoft.2021.105257
- Iqbal, N., Khan, A. N., Rizwan, A., Ahmad, R., Kim, B. W., Kim, K., et al. (2021). Groundwater level prediction model using correlation and difference mechanisms based on boreholes data for sustainable hydraulic resource management. *IEEE Access* 9, 96092–96113. doi:10.1109/access.2021.3094735
- Jafari, H., Bagheri, R., Forghani, G., and Esmaeili, M. (2015). The consequences of disposing wastewater in an endorheic wetland in southwest Iran. *Environ. Monit. Assess.* 187, 1–14. doi:10.1007/s10661-015-4560-0
- Kalantari, N., Pawar, N. J., and Keshavarzi, M. R. (2009). Water resource management in the intermountain Izeh plain, southwest of Iran. *J. Mt. Sci.* 6, 25–41. doi:10.1007/s11629-009-0212-6
- Kang, D.-h., So, Y. H., Kim, I. K., Oh, S.-b., Kim, S., and Kim, B.-W. (2017). Groundwater flow and water budget analyses using HydroGeoSphere model at the facility agricultural complex. *J. Eng. Geol.* 27, 313–322. doi:10.9720/kseg.2017.3.313
- Kanjo, E., Younis, E. M. G., and Ang, C. S. (2019). Deep learning analysis of mobile physiological, environmental and location sensor data for emotion detection. *Inf. Fusion* 49, 46–56. doi:10.1016/j.inffus.2018.09.001
- Kaya, Y. Z., Üneş, F., Demirci, M., Taşar, B., and Varçin, H. (2018). "Groundwater level prediction using artificial neural network and M5 tree models," in Air and Water Components of the Environment Conference, March, 2018, 195–201.
- Kecman, V. (2001). *Learning and soft computing: support vector machines, neural networks, and fuzzy logic models*. Cambridge, Massachusetts, United States: MIT press.
- Khan, J., Lee, E., Balobaid, A. S., and Kim, K. (2023). A comprehensive review of conventional, machine learning, and deep learning models for groundwater level (GWL) forecasting. *Appl. Sci.* 13, 2743. doi:10.3390/app13042743
- Khan, U. T., and Valeo, C. (2016). Dissolved oxygen prediction using a possibility theory based fuzzy neural network. *Hydrology Earth Syst. Sci.* 20, 2267–2293. doi:10.5194/hess-20-2267-2016
- Kim, I., Park, D., Kyung, D., Kim, G., Kim, S., and Lee, J. (2016). Comparative influences of precipitation and river stage on groundwater levels in near-river areas. *Sustainability* 8 (1), 1. doi:10.3390/su8010001
- Kombo, O. H., Kumaran, S., Sheikh, Y. H., Bovim, A., and Jayavel, K. (2020). Long-term groundwater level prediction model based on hybrid KNN-RF technique. *Hydrology* 7, 59. doi:10.3390/hydrology7030059
- Kotsiantis, S. B. (2013). Decision trees: a recent overview. *Artif. Intell. Rev.* 39, 261–283. doi:10.1007/s10462-011-9272-4
- Kumar, D., and Ahmed, S. (2003). Seasonal behaviour of spatial variability of groundwater level in a granitic aquifer in monsoon climate. *Curr. Sci.*, 188–196.
- Kumar, D., Roshni, T., Singh, A., Jha, M. K., and Samui, P. (2020). Predicting groundwater depth fluctuations using deep learning, extreme learning machine and Gaussian process: a comparative study. *Earth Sci. Inf.* 13, 1237–1250. doi:10.1007/s12145-020-00508-y
- Li, D., Chen, D., Jin, B., Shi, L., Goh, J., and Ng, S.-K. (2019). *MAD-GAN: multivariate anomaly detection for time series data with generative adversarial networks*. Berlin, Germany: Springer, 703–716.
- Lin, H., Gharehbaghi, A., Zhang, Q., Band, S. S., Pai, H. T., Chau, K. W., et al. (2022). Time series-based groundwater level forecasting using gated recurrent unit deep neural networks. *Eng. Appl. Comput. Fluid Mech.* 16 (1), 1655–1672. doi:10.1080/19942060.2022.2104928
- Ma, J., Liu, H., Shi, Y., and Zhang, H. (2022). "Study on the numerical simulation of groundwater "drainage and recharge" in open pit coal mine based on FEFLOW," in 2022 8th International Conference on Hydraulic and Civil Engineering: Deep Space Intelligent Development and Utilization Forum (ICHCE), Xi'an, China, November, 2022, 1–8.
- Machiwal, D., and Singh, P. K. (2015). Understanding factors influencing groundwater levels in hard-rock aquifer systems by using multivariate statistical techniques. *Environ. Earth Sci.* 74 (7), 5639–5652. doi:10.1007/s12665-015-4578-1
- Mahdavi, P., Kharazi, H. G., Eslami, H., Zohrabi, N., and Razaz, M. (2021). Drought occurrence under future climate change scenarios in the Zard River basin, Iran. *Water Supply* 21 (2), 899–917. doi:10.2166/ws.2020.367
- Malakar, P., Mukherjee, A., Bhanja, S. N., Sarkar, S., Saha, D., and Ray, R. K. (2021). Deep learning-based forecasting of groundwater level trends in India: implications for crop production and drinking water supply. *ACS ES&T Eng.* 1, 965–977. doi:10.1021/acestengg.0c00238
- Marchant, B., Mackay, J., and Bloomfield, J. (2016). Quantifying uncertainty in predictions of groundwater levels using formal likelihood methods. *J. Hydrology* 540, 699–711. doi:10.1016/j.jhydrol.2016.06.014
- Ming, Y., Cao, S., Zhang, R., Li, Z., Chen, Y., Song, Y., et al. (2017). "Understanding hidden memories of recurrent neural networks," in 2017 IEEE Conference on Visual Analytics Science and Technology (VAST), Phoenix, AZ, USA, October, 2017, 13–24.
- Mirsalari, S. A., Sinaei, S., Salehi, M. E., and Daneshlab, M. (2020). "MuBiNN: multi-level binarized recurrent neural network for EEG signal classification," in 2020 IEEE International Symposium on Circuits and Systems (ISCAS), Seville, Spain, October, 2020, 1–5.
- Mohammed, K. S., Shabanlou, S., Rajabi, A., Yosefvand, F., and Izadbakhsh, M. A. (2023). Prediction of groundwater level fluctuations using artificial intelligence-based models and GMS. *Appl. Water Sci.* 13, 54. doi:10.1007/s13201-022-01861-7
- Mukherjee, A., and Ramachandran, P. (2018). Prediction of GWL with the help of GRACE TWS for unevenly spaced time series data in India: analysis of comparative performances of SVR, ANN and LRM. *J. hydrology* 558, 647–658. doi:10.1016/j.jhydrol.2018.02.005
- Nadiri, A. A., Chitsazan, N., Tsai, F. T. C., and Moghaddam, A. A. (2014). Bayesian artificial intelligence model averaging for hydraulic conductivity estimation. *J. Hydrologic Eng.* 19, 520–532. doi:10.1061/(asce)he.1943-5584.0000824
- Nadiri, A. A., Fijani, E., Tsai, F. T. C., and Asghari Moghaddam, A. (2013). Supervised committee machine with artificial intelligence for prediction of fluoride concentration. *J. Hydroinformatics* 15, 1474–1490. doi:10.2166/hydro.2013.008
- Nassery, H. R., Aljani, F., and Mirzaei, L. (2009). Environmental characterization of a karst polje: an example from Izeh polje, southwest Iran. *Environ. Earth Sci.* 59, 99–108. doi:10.1007/s12665-009-0008-6
- Nayak, P. C., Rao, Y. R. S., and Sudheer, K. P. (2006). Groundwater level forecasting in a shallow aquifer using artificial neural network approach. *Water Resour. Manag.* 20, 77–90. doi:10.1007/s11269-006-4007-z
- O'Shea, K., and Nash, R. (2015). An introduction to convolutional neural networks. <https://arxiv.org/abs/1511.08458>.
- Osman, A. I. A., Ahmed, A. N., Chow, M. F., Huang, Y. F., and El-Shafie, A. (2021). Extreme gradient boosting (Xgboost) model to predict the groundwater levels in Selangor Malaysia. *Ain Shams Eng. J.* 12, 1545–1556. doi:10.1016/j.asej.2020.11.011

- Ozer, M. E., Sarica, P. O., and Arga, K. Y. (2020). New machine learning applications to accelerate personalized medicine in breast cancer: rise of the support vector machines. *Omics a J. Integr. Biol.* 24, 241–246. doi:10.1089/omi.2020.0001
- Panahi, M., Sadhasivam, N., Pourghasemi, H. R., Rezaie, F., and Lee, S. (2020). Spatial prediction of groundwater potential mapping based on convolutional neural network (CNN) and support vector regression (SVR). *J. Hydrology* 588, 125033. doi:10.1016/j.jhydrol.2020.125033
- Pham, Q. B., Kumar, M., Di Nunno, F., Elbeltagi, A., Granata, F., Islam, A. R. M. T., et al. (2022). Groundwater level prediction using machine learning algorithms in a drought-prone area. *Neural Comput. Appl.* 34, 10751–10773. doi:10.1007/s00521-022-07009-7
- Pragnaditya, M., Abhijit, M., Bhanja, S. N., Kumar, R. R., Sudeshna, S., and Anwar, Z. (2021). Machine-learning-based regional-scale groundwater level prediction using GRACE. *Hydrogeology J.* 29, 1027–1042. doi:10.1007/s10040-021-02306-2
- Priyan, K. (2021). Issues and challenges of groundwater and surface water management in semi-arid regions. *Groundw. Resour. Dev. Plan. Semi-Arid Region*, 1–17. doi:10.1007/978-3-030-68124-1_1
- Rajae, T., Ebrahimi, H., and Nourani, V. (2019). A review of the artificial intelligence methods in groundwater level modeling. *J. hydrology* 572, 336–351. doi:10.1016/j.jhydrol.2018.12.037
- Rashidi, M., and Hosseinzadeh, M. M. (2019). The role of sub-basins overlooking the city in the occurrence of urban floods in Izeh (Khuzestan). *J. Geogr. Environ. Hazards* 8 (1), 25–42. doi:10.22067/geo.v0i0.78855
- Rathinasamy, M., Khosa, R., Adamowski, J., Ch, S., Partheepan, G., Anand, J., et al. (2014). Wavelet-based multiscale performance analysis: an approach to assess and improve hydrological models. *Water Resour. Res.* 50, 9721–9737. doi:10.1002/2013wr014650
- Russo, S. L., and Taddia, G. (2009). Groundwater in the urban environment: management needs and planning strategies. *Am. J. Environ. Sci.* 5, 494–500. doi:10.3844/ajessp.2009.494.500
- Samantaray, S., Biswakalyani, C., Singh, D. K., Sahoo, A., and Prakash Satapathy, D. (2022). Prediction of groundwater fluctuation based on hybrid ANFIS-GWO approach in arid Watershed, India. *Soft Comput.* 26 (11), 5251–5273. doi:10.1007/s00500-022-07097-6
- Seifi, A., Ehteram, M., Singh, V. P., and Mosavi, A. (2020). Modeling and uncertainty analysis of groundwater level using six evolutionary optimization algorithms hybridized with ANFIS, SVM, and ANN. *Sustainability* 12 (10), 4023. doi:10.3390/su12104023
- Sharafati, A., Asadollah, S. B. H. S., and Neshat, A. (2020). A new artificial intelligence strategy for predicting the groundwater level over the Rafsanjan aquifer in Iran. *J. Hydrology* 591, 125468. doi:10.1016/j.jhydrol.2020.125468
- Shi, H., Xu, M., and Li, R. (2017). Deep learning for household load forecasting—a novel pooling deep RNN. *IEEE Trans. Smart Grid* 9, 5271–5280. doi:10.1109/tsg.2017.2686012
- Singh, A., Patel, S., Bhadani, V., Kumar, V., and Gaurav, K. (2024). AutoML-GWL: automated machine learning model for the prediction of groundwater level. *Eng. Appl. Artif. Intell.* 127, 107405. doi:10.1016/j.engappai.2023.107405
- Singh, S. K. (2015). Groundwater arsenic contamination in the Middle-Gangetic Plain, Bihar (India): the danger arrived. *Int. Res. J. Environ. Sci.* 4 (2), 70–76.
- Singh, S. K., Shirzadi, A., and Pham, B. T. (2021a). Application of artificial intelligence in predicting groundwater contaminants. *Water Pollut. Manag. Pract.*, 71–105. doi:10.1007/978-981-15-8358-2_4
- Singh, S. K., Shirzadi, A., and Pham, B. T. (2021b). Application of artificial intelligence in predicting groundwater contaminants. *Water Pollut. Manag. Pract.*, 71–105. doi:10.1007/978-981-15-8358-2_4
- Sit, M., Demiray, B. Z., Xiang, Z., Ewing, G. J., Sermet, Y., and Demir, I. (2020). A comprehensive review of deep learning applications in hydrology and water resources. *Water Sci. Technol.* 82 (12), 2635–2670. doi:10.2166/wst.2020.369
- Sun, J., Hu, L., Li, D., Sun, K., and Yang, Z. (2022). Data-driven models for accurate groundwater level prediction and their practical significance in groundwater management. *J. Hydrology* 608, 127630. doi:10.1016/j.jhydrol.2022.127630
- Szandała, T. (2021). Review and comparison of commonly used activation functions for deep neural networks. *Bio-inspired neurocomputing*, 203–224. doi:10.1007/978-981-15-5495-7_11
- Tao, H., Hameed, M. M., Marhoon, H. A., Zounemat-Kermani, M., Heddam, S., Kim, S., et al. (2022a). Groundwater level prediction using machine learning models: a comprehensive review. *Neurocomputing* 489, 271–308. doi:10.1016/j.neucom.2022.03.014
- Tao, H., Hameed, M. M., Marhoon, H. A., Zounemat-Kermani, M., Salim, H., Sungwon, K., et al. (2022b). Groundwater level prediction using machine learning models: a comprehensive review. *Neurocomputing* 489, 271–308. doi:10.1016/j.neucom.2022.03.014
- Trefry, M. G., and Muffels, C. (2007). FEFLOW: a finite-element ground water flow and transport modeling tool. *Groundwater* 45, 525–528. doi:10.1111/j.1745-6584.2007.00358.x
- Wang, C., Bai, Y., Yuan, H., Liu, J., Fernández-Ontiveros, J. A., Coelho, P. R. T., et al. (2022). J-PLUS: support vector regression to measure stellar parameters. *Astronomy Astrophysics* 664, A38. doi:10.1051/0004-6361/202243130
- Wang, J., Lin, J., and Wang, Z. (2017). Efficient hardware architectures for deep convolutional neural network. *IEEE Trans. Circuits Syst. I Regul. Pap.* 65, 1941–1953. doi:10.1109/tcsi.2017.2767204
- Wang, S., Shao, J., Song, X., Zhang, Y., Huo, Z., and Zhou, X. (2008). Application of MODFLOW and geographic information system to groundwater flow simulation in North China Plain, China. *Environ. Geol.* 55, 1449–1462. doi:10.1007/s00254-007-1095-x
- Wang, Y., Feng, B., and Ding, Y., 2021. DSXplore: optimizing convolutional neural networks via sliding-channel convolutions. 2021 IEEE International Parallel and Distributed Processing Symposium (IPDPS), Portland, OR, USA, May, 2021, pp. 619–628.
- Wen, X., Feng, Q., Deo, R. C., Wu, M., and Si, J. (2017). Wavelet analysis–artificial neural network conjunction models for multi-scale monthly groundwater level predicting in an arid inland river basin, northwestern China. *Hydrology Res.* 48, 1710–1729. doi:10.2166/nh.2016.396
- Worsa-Kozak, M., Zimroz, R., Michalak, A., Wolkersdorfer, C., Wylomańska, A., and Kowalczyk, M. (2020). Groundwater level fluctuation analysis in a semi-urban area using statistical methods and data mining techniques—a case study in wroclaw, Poland. *Appl. Sci.* 10 (10), 3553. doi:10.3390/app10103553
- Wu, Z., Lu, C., Sun, Q., Lu, W., He, X., Qin, T., et al. (2023). Predicting groundwater level based on machine learning: a case study of the hebei plain. *Water* 15 (4), 823. doi:10.3390/w15040823
- Yamashita, R., Nishio, M., Do, R. K. G., and Togashi, K. (2018). Convolutional neural networks: an overview and application in radiology. *Insights into imaging* 9, 611–629. doi:10.1007/s13244-018-0639-9
- Yoon, H., Jun, S. C., Hyun, Y., Bae, G. O., and Lee, K. K. (2011). A comparative study of artificial neural networks and support vector machines for predicting groundwater levels in a coastal aquifer. *J. hydrology* 396 (1–2), 128–138. doi:10.1016/j.jhydrol.2010.11.002
- Yosefvand, F., and Shabanlou, S. (2020). Forecasting of groundwater level using ensemble hybrid wavelet–self-adaptive extreme learning machine-based models. *Nat. Resour. Res.* 29 (5), 3215–3232. doi:10.1007/s11053-020-09642-2
- Zhang, H., Shi, Z., Wang, G., Sun, X., Yan, R., and Liu, C. (2019). Large earthquake reshapes the groundwater flow system: insight from the water-level response to earth tides and atmospheric pressure in a deep well. *Water Resour. Res.* 55, 4207–4219. doi:10.1029/2018wr024608
- Zhang, J., Zhu, Y., Zhang, X., Ye, M., and Yang, J. (2018). Developing a Long Short-Term Memory (LSTM) based model for predicting water table depth in agricultural areas. *J. hydrology* 561, 918–929. doi:10.1016/j.jhydrol.2018.04.065
- Ziyari, K., and Latifi, O. (2022). An analysis of land ecological networks in Izeh city using colonial competition algorithm. *Urban Struct. Funct. Stud.* 9 (30), 127–147. doi:10.22080/USFS.2021.3517